Acta Pharmaceutica Sinica B 2017;7(1):73–79

Chinese Pharmaceutical Association
Institute of Materia Medica, Chinese Academy of Medical Sciences

Acta Pharmaceutica Sinica B

www.elsevier.com/locate/apsb
www.sciencedirect.com

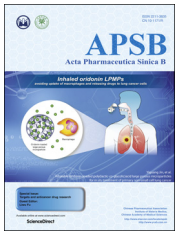

ORIGINAL ARTICLE

2,3-Diaryl-3*H*-imidazo[4,5-*b*]pyridine derivatives as potential anticancer and anti-inflammatory agents

Erin Marie Kirwen[a,†], Tarun Batra[b,†], Chandrabose Karthikeyan[b], Girdhar Singh Deora[c], Vandana Rathore[c,d,e], Chaitanya Mulakayala[f], Naveen Mulakayala[g], Amy Catherine Nusbaum[a], Joel Chen[a], Haneen Amawi[a], Kyle McIntosh[a], Sahabjada[h], Neelam Shivnath[h], Deepak Chowarsia[b], Nisha Sharma[i], Md Arshad[h], Piyush Trivedi[b,*], Amit K. Tiwari[a,]**

[a]*Department of Pharmacology and Experimental Therapeutics, College of Pharmacy & Pharmaceutical Sciences, University of Toledo, Toledo, OH 43614, USA*
[b]*School of Pharmaceutical Sciences, Rajiv Gandhi Technical University, Gandhi Nagar, Bhopal, MP 462036, India*
[c]*The University of Queensland, School of Pharmacy, Brisbane, Qld 4072, Australia*
[d]*Dr. Reddy's Institute of Life Sciences, University of Hyderabad Campus, Gachibowli, Hyderabad 500046, India*
[e]*The University of Queensland, School of Biomedical Sciences, Brisbane, Qld 4072, Australia*
[f]*Department of Biosciences, Sri Satya Sai Institute of Higher Learning, Anantapur campus, Andhra Pradesh 515001, India*
[g]*Clearsynth Labs Ltd., Research Centre, IDA-Mallapur, Hyderabad 500076, India*
[h]*Molecular Endocrinology Lab, Department of Zoology, University of Lucknow, Lucknow, UP 226007, India*
[i]*University Institute of Pharmacy, Chhatrapati Shahu Ji Maharaj University, Kanpur, UP 208024, India*

Received 7 April 2016; received in revised form 14 May 2016; accepted 17 May 2016

*Corresponding author. Tel.: +91755 2678883.
**Corresponding author. Tel.: +1 419 973 1961; fax: +1419 383 1909.
E-mail addresses: piyush.trivedi@rgtu.net (Piyush Trivedi), amit.tiwari@utoledo.edu (AmitK Tiwari).
†These authors made equal contributions to this work.

Peer review under responsibility of Institute of Materia Medica, Chinese Academy of Medical Sciences and Chinese Pharmaceutical Association.

http://dx.doi.org/10.1016/j.apsb.2016.05.003

KEY WORDS

3*H*-Imidazo[4,5-*b*]pyridine;
Cytotoxicity;
MTT assay;
COX inhibitors;
Docking studies

Abstract In this study we examined the suitability of the *3H*-imidazo[4,5-*b*]pyridine ring system in developing novel anticancer and anti-inflammatory agents incorporating a diaryl pharmacophore. Eight 2,3-diaryl-3*H*-imidazo[4,5-*b*]pyridine derivatives retrieved from our in-house database were evaluated for their cytotoxic activity against nine cancer cell lines. The results indicated that the compounds showed moderate cytotoxic activity against MCF-7, MDA-MB-468, K562 and SaOS2 cells, with K562 being the most sensitive among the four cancer cell lines. The eight 2,3-diaryl-3*H*-imidazo[4,5-*b*]pyridine derivatives were also evaluated for their COX-1 and COX-2 inhibitory activity *in vitro*. The results showed that compound **3f** exhibited 2-fold selectivity with IC_{50} values of 9.2 and 21.8 μmol/L against COX-2 and COX-1, respectively. Molecular docking studies on the most active compound **3f** revealed a binding mode similar to that of celecoxib in the active site of the COX-2 enzyme.

1. Introduction

Heterocycles with a vicinal diaryl substitution are an important pharmacophore in medicinal chemistry and are key building blocks for a variety of compounds showing anticancer and anti-inflammatory activities[1,2]. The cytotoxic properties of these compounds are mainly attributed to tubulin inhibition whereas their anti-inflammatory activity is predominantly elicited through the inhibition of cyclooxygenase (COX) enzymes (Fig. 1A)[1,3]. Both activities require the diaryl pharmacophore with a *cis*-olefin configuration[4]. Hence, several aromatic heterocyclic rings including five-membered (pyrazole[5], Imidazole[6], thiazole[5], furazan (1,2,5-oxadiazole)[7], oxazole[6], isoxazole[8], 1,2,3-thiadiazole[9], triazole[10]), six-membered (pyridine) and fused bicyclic rings, like pyrazolo[1,5-*a*]pyrimidines[11], quinazolinone, benzimidazole, indole[12], benzothiophene[7] and benzofuran[7], have been investigated as a heterocyclic core in stabilizing the *cis*-olefin orientation of the two aryl rings (Fig. 1A). 3*H*-imidazo[4,5-*b*]pyridine represents an interesting class of heterocyclic core for the design of diaryl derivatives with anticancer and anti-inflammatory activities. Motivated by the above observations, the present research strives to examine the utility of 3*H*-imidazo[4,5-*b*]pyridine as a heterocyclic bridge for the design of novel 2,3-diaryl-3*H*-imidazo [4,5-*b*]pyridine derivatives with anticancer and anti-inflammatory activities. Eight compounds with either OH, OCH_3 or both, or CF_3 in aryl ring A and halo (F and Cl) or OCH_3 substitution in aryl ring B, were retrieved from our in-house database (Fig. 1B) and tested for anticancer activity against a panel of nine cancer cell lines (breast, prostate, colon, blood and bone cancer) and two non-cancerous cell lines. The eight compounds were also evaluated for their inhibitory on COX-1 and COX-2 enzymes. To the best our knowledge, the cytotoxic and anti-inflammatory potential of this class of compounds have not been reported in literature.

2. Results and discussion

2.1. Chemistry

Diaryl substituted 3*H*-imidazo[4,5-*b*]pyridine derivatives were previously synthesized in our laboratory using a one pot synthetic protocol from the corresponding *N*-aryl nitropyridines as shown in Scheme 1[12]. The requisite 3-nitro-*N*-aryl pyridin-2-amines (**2a–c**) were prepared *in situ* by heating a mixture of 2-chloro-3-nitropyridine (**1a**) and substituted anilines in DMSO at 100 °C. Subsequent treatment of the DMSO solution of the resulting 3-nitro-*N*-phenyl-pyridin-2-amine with aromatic aldehydes and sodium dithionite at 80 °C afforded the titled compounds in moderate to good yields. The structures assigned to the compounds were supported by the data obtained from IR, ^{1}H NMR and mass spectral studies.

2.2. Cytotoxicity studies

The cytotoxic activity of eight diaryl substituted 3*H*-imidazo[4,5-*b*]pyridine derivatives was evaluated against nine cancer cell lines and two non-cancerous cell lines using the MTT assay. For many of the cell lines, the concentration of the compounds had to be over 100 μmol/L for any cell death to occur. For the prostate cancer cell line DU-145, lung cancer cell line A549, and breast cancer cell line MDAMB-231, none of the eight compounds showed any effect as in Table 1. Minimal cell death was seen in the pancreatic cancer cell line PANC-1, with compounds **3g** and **3h** having an IC_{50} of 83.54 and 57.69 μmol/L, respectively. Only compound **3h** had an effect on the colon cancer cell line HCT-15 with an IC_{50} of 66.92 μmol/L. The cancer cell lines that had the most cell growth inhibition were MCF-7, MDA-MB-468, K562 and SaOS2. The compounds showed maximal growth inhibitory potency against K562 with IC_{50} values ranging from 42 to 57 μmol/L. In the case of MCF-7 and SaOS2, growth inhibition was observed at concentration ranging from 44 to 72 μmol/L and 52.5 to 71.5 μmol/L, respectively. Three compounds **3b**, **3e** and **3g** showed modest inhibition of MDA-MB-468 cell growth with IC_{50} values of 66.46, 78.82 and 69.34 μmol/L, respectively. The mouse fibroblast cell line KB-31 also had effects with IC_{50} values of **3b** of 74.96 μmol/L, **3e** of 95.58 μmol/L, **3g** of 64.36 μmol/L and **3h** of 70.91 μmol/L. The normal cell line used was HEK 293 and only one of the compounds in the series, **3h**, caused cell death with an IC_{50} of 80 μmol/L.

2.3. COX inhibition studies

In addition to cytotoxic activity, the eight compounds were also evaluated for COX-1 and COX-2 inhibitory activity as diaryl pharmacophore is also an integral component of several COX

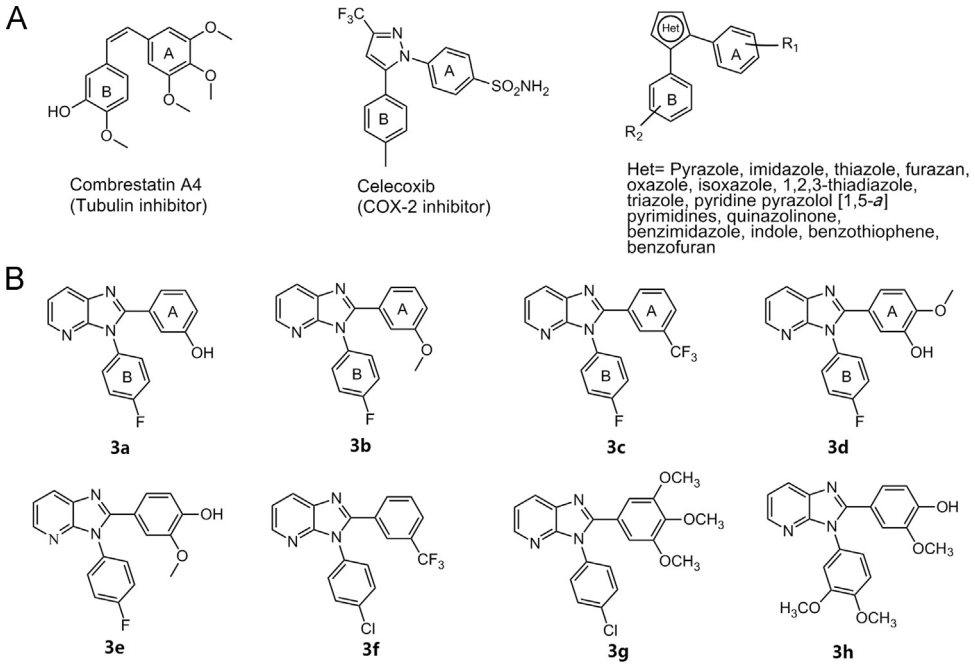

Figure 1 (A) Structures of some biologically active molecules with diaryl pharmacophore and different heterocyclic scaffolds employed for stabilizing the '*cis*' diaryl configuration in literature; (B) Structures of molecules 2,3-diaryl-3*H*-imidazo[4,5-*b*]pyridine derivatives evaluated in this study.

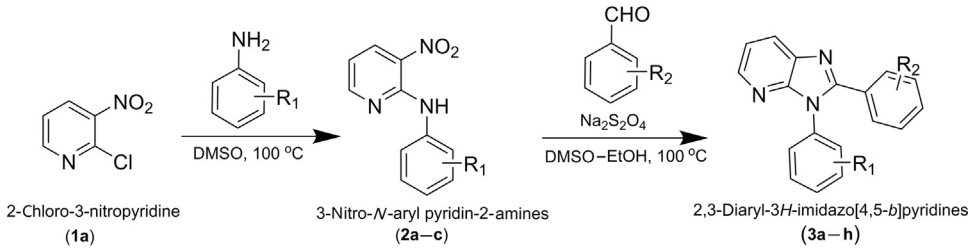

Scheme 1 Synthesis of 2,3-diaryl-*3H*-imidazo[4,5-*b*]pyridine derivatives (**3a**–**3h**).

inhibitors. The COX inhibition as given by IC_{50} values in Table 2 clearly demonstrate the effectiveness of all 3*H*-imidazo[4,5-*b*]pyridine derivatives against both COX-1 and COX-2 enzymes. The compounds inhibited COX-1 with IC_{50} values ranging from 10 to 43 µmol/L, whereas COX-2 inhibition was observed in concentration ranging from 9.2 to 279.3 µmol/L. Most notably, structural variations in both aryl rings appeared to affect both the potency and selectivity of these analogues against these enzymes. This is a desirable trait especially for the development of clinically useful anti-inflammatory agents targeting the COX-2 enzyme. Compound **3f** with a 4-chloro substitution in the *N*-phenyl ring and a 3-CF_3 substitution in the 2-phenyl ring was found to be the most active (COX-2, IC_{50} = 9.2 µmol/L) in the series. Compounds **3c** that had 4-fluoro and 3-CF_3 substitutions on the *N*-phenyl and 2-phenyl rings, respectively and compound **3h** that possessed 3,4-dimethoxyl and 3-OCH_3, 4-OH substituents in the same positions exhibited the modest COX-2 inhibitory activity ($IC_{50} \approx 15$ µmol/L).

2.4. *Docking studies*

Molecular docking studies were proposed for compound **3f** in order to rationalize its potency and selectivity against COX-2. Prior to docking studies with compound **3f**, the glide docking protocol was validated by evaluating the ability to reproduce the binding conformation of the co-crystallized ligand celecoxib. The docking protocol followed was found reliable as the root mean square deviation (RMSD) between the predicted conformation and the observed X-ray crystallographic conformation of the celecoxib (PDB ID: 3LN1) was found to be 0.33 Å. The binding mode predicted for **3f** in the docking studies is shown in Fig. 2A. The binding mode observed for **3f** is very similar to the one observed for the co-crystallized celecoxib (Fig. 2B). The docked structures of **3f** and celecoxib were oriented so that the *N*-phenyl ring of **3f** overlapped with that of 4-sulfamoylphenyl ring in celecoxib in the selectivity pocket of COX-2 and the 3*H*-imidazo[4,5-*b*]pyridine ring overlapped with the trifluoromethyl substituted pyrazolyl ring in celecoxib. Furthermore, the chlorine atom at the *p*-position of the *N*-phenyl ring is favorably placed in the selectivity pocket facilitating electrostatic interactions with Arg499 and Phe504. However, the 2-phenyl ring in **3f** is more planar in comparison to the second phenyl ring in celecoxib, resulting in a partial overlap of both these rings. This deviation in the orientation of the 2-phenyl ring might serve to accommodate the 3-trifluoromethyl substitution in the hydrophobic pocket formed by Phe367, Leu370, Trp373 and Met508. Nevertheless, the binding parallels observed

Table 1 Cytotoxic activity of 2,3-diaryl-3*H*-imidazo[4,5-*b*]pyridine derivatives against various cell lines (cancerous and non-cancerous).

Compd.	IC_{50} (μmol/L)					
	Breast			Prostate	Pancreas	
	MCF-7	MDAMB-231	MDAMB-468	DU-145	PANC-1	
3a	61.5	>100	>100	>100	>100	
3b	69	>100	66.46	>100	>100	
3c	44	>100	>100	>100	>100	
3d	72	>100	>100	>100	>100	
3e	60	>100	78.82	>100	>100	
3f	49.9	>100	>100	>100	>100	
3g	56	>100	69.34	>100	83.54	
3h	53	>100	>100	>100	57.69	
Compd.	IC_{50} (μmol/L)					
	Blood	Bone	Colon	Lung	Normal	Mouse fibroblast
	K562	SaoS2	HCT15	A549	HEK293	KB-31
3a	49	64	>100	>100	>100	>100
3b	46	67	>100	>100	>100	74.96
3c	42	52.5	>100	>100	>100	>100
3d	57	71.5	>100	>100	>100	>100
3e	53	62.5	>100	>100	>100	95.58
3f	43	53.5	>100	>100	>100	>100
3g	47	55	>100	>100	>100	64.36
3h	54.5	59	66.92	>100	80	70.91

Table 2 COX inhibition data of 2,3-diaryl-3*H*-imidazo[4,5-*b*]pyridine derivatives.

Compd.	IC_{50} (μmol/L)		Selectivity ratio
	COX-1	COX-2	COX-2/COX-1
3a	10.0±0.01	35.9±2.0	3.59
3b	15.0±0.13	NA	NA
3c	36.0±1.4	15.1±0.9	0.42
3d	42.7±2.5	25.6±1.0	0.60
3e	16.8±0.1	279.3±7.2	16.58
3f	21.8±1.1	9.2±0.02	0.42
3g	19.1±0.3	22.4±2.5	1.17
3h	18.5±0.00	15.4±3.1	0.83
Indomethacin	0.0067±0.00	0.048±0.00	7.16
Celecoxib	15±0.6	0.042±0.00	0.0028

NA: not achieved at the tested concentrations.

between celecoxib and **3f** may rationalize the inhibitory potency shown by the compound against COX-2 enzyme.

3. Conclusions

The present study is an attempt to examine the suitability of 3*H*-imidazo[4,5-*b*]pyridine as a heterocyclic core for the development of anticancer and anti-inflammatory molecules incorporating a diaryl pharmacophore. Eight 1,2-diaryl-3*H*-imidazo[4,5-*b*]pyridines retrieved from our in-house database were evaluated for their cytotoxic activity against nine cancer cell lines and COX (1 and 2) inhibitory activity *in vitro*. The compounds showed moderate cytotoxicity against MCF-7, MDA-MB-468, K562, and SaOS2 cells with K562 being the most sensitive among the four cancer cell lines. The compounds also exerted inhibitory activity against both the COX-1 and COX-2 enzymes. Most interesting was compounds **3c**, **3f** and **3h,** which showed potent (IC_{50} < 20 μmol/L) and selective COX-2 inhibition. The docking study of the most active analogue **3f** into the COX-2 active site supported the *in vitro* potency shown by the compound and also revealed the nature of the interactions between the molecule and amino acid residues in the active site of COX-2. Taken together, these promising findings established 1,2-diaryl-3*H*-imidazo[4,5-*b*]pyridines as a promising scaffold in developing anticancer and anti-inflammatory agents.

4. Experimental

4.1. Chemistry

All chemicals and solvents used in this study were purchased locally from commercial suppliers and were used without further purification. Melting points were determined on a Veego Digital Melting Point apparatus in open capillaries and have not been corrected. The ^{1}H NMR spectra were recorded on in DMSO-d_6 on a Bruker Avance II 400 MHz spectrometer. Chemical shifts were recorded in parts per million (ppm) and were reported relative to tetramethylsilane (TMS). The infrared (IR) spectra were recorded on a Schimadzu IR Prestige-21 FTIR spectrophotometer in KBr. Mass spectra were recorded on an Applied Biosystem QTRAP 3200 MS/MS system in ESI mode.

4.1.1. Synthesis of 2,3-diaryl-3H-imidazo[4,5-b]pyridine derivatives (**3a**–**3h**)

The synthesis of 2,3-diaryl-3*H*-imidazo[4,5-*b*]pyridine derivatives (**3a**–**3h**) was performed according to a reported literature procedure[13].

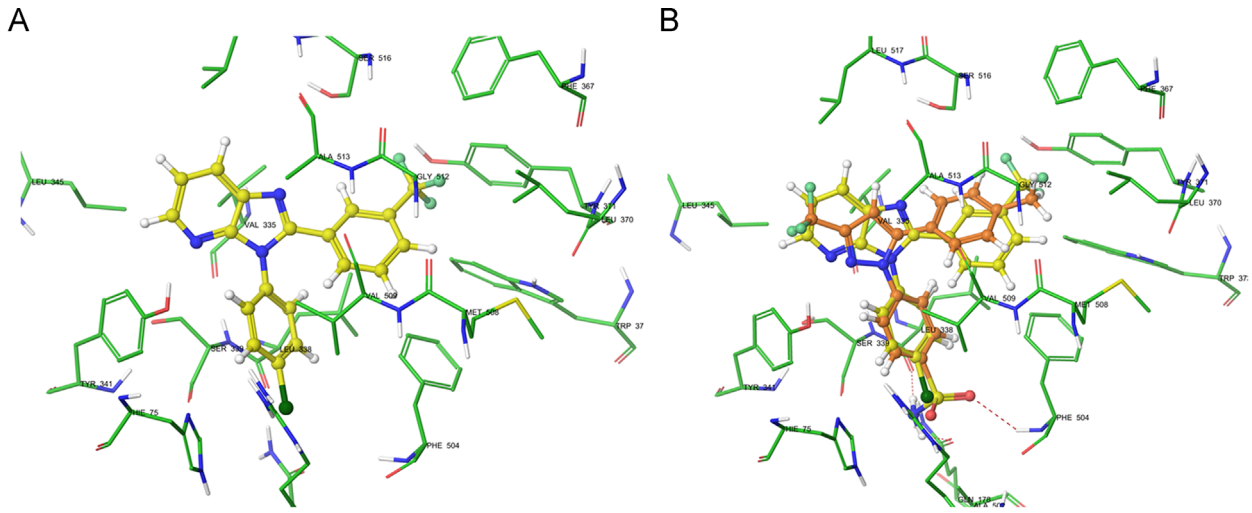

Figure 2 (A) XP-Glide predicted binding mode of **3f** in the active site of COX-2 (PDB ID: 3LN1); (B) Overlay of docked conformation of **3f** on docked conformation of celecoxib (yellow) in the active site of COX-2. Important amino acids are depicted as sticks with the atoms colored as carbon (green), hydrogen (white), nitrogen (blue), oxygen (red), sulfur (yellow), whereas the ligands are shown with the same color scheme as above except for carbon atoms are represented in yellow for **3f** and orange for celecoxib. Fluorine atoms in **3f** are represented in light green and chlorine atom is represented in dark green. Red dotted lines represent hydrogen bonding.

***3-(3-(4-Fluorophenyl)-3H-imidazo[4,5-b]pyridin-2-yl)phenol (3a)*:** Yield 44%; m.p. 235–236 °C; FT-IR (KBr) υ (cm^{-1}): 3184 (O-H), 3059 (aromatic C-H), 1589 (C=N), 1388 (C-N), 1224 (C-F), 1159 (C-O); ^{1}H NMR (400 MHz, DMSO-d_6) δ 9.35 (s, 1H, ArOH), 8.26 (d, 1H, J=4.72 Hz, ArH), 8.05 (d, 1H, J=8.0 Hz, ArH), 7.38–7.35 (m, 2H, ArH), 7.29–7.26 (m, 1H, ArH), 7.18 (t, 2H, J=8.52 Hz, ArH), 7.08 (t, 1H, J=7.92 Hz, ArH), 7.03 (s, 1H, ArH), 6.88 (d, 1H, J=7.72 Hz, ArH), 6.84 (d, 1H, J=4.12 Hz, ArH); MS-API: $[M+H]^+$ 306 (Calcd. 305.10).

***3-(4-Fluorophenyl)-2-(3-methoxyphenyl)-3H-imidazo[4,5-b]pyridine (3b)*:** Yield 57%; m.p. 236–237 °C; FT-IR (KBr) υ (cm^{-1}): 3053 (C-H aromatic), 2955 (methyl C-H), 1593 (C=N), 1381 (C-N), 1230 (C-F), 1251, 1033 (C-O-C); ^{1}H NMR (400 MHz, DMSO-d_6): δ 8.39 (d, 1H, J=4.8 Hz, ArH), 8.16 (d, 1H, J=8.04 Hz, ArH), 7.39–7.36 (m, 2H, ArH), 7.33–7.30 (m, 1H, ArH), 7.26–7.18 (m, 4H, ArH), 7.125–7.09 (m, 1H, ArH), 6.97–6.95 (m, 1H, ArH), 3.74 (s, 3H, -OCH_3); MS-API: $[M+H]^+$ 320 (Calcd. 319.11).

3-(4-Fluorophenyl)-2-(3-(trifluoromethyl)phenyl)-3H-imidazo[4,5-b]pyridine (3c): Yield 26%; m.p. 185–187 °C; FT-IR (KBr) υ (cm^{-1}): 3068 (aromatic C-H), 1599 (C=N), 1383 (C-N), 1228 (C-F,CF_3), 1185 (C-F); ^{1}H NMR (400 MHz, DMSO-d_6): δ 8.43 (d, 1H, J=4.76 Hz, ArH), 8.19 (d, 1H, J=9.2 Hz, ArH), 7.96 (s, 1H, ArH), 7.72–7.66 (m, 2H, ArH), 7.47 (t, 1H, J=7.92 Hz, ArH), 7.39–7.34 (m, 3H, ArH), 7.27–7.22 (m, 1H, ArH); MS-API: $[M+H]^+$ 358 (Calcd. 357.1).

***4-(3-(4-Fluorophenyl)-3H-imidazo[4,5-b]pyridin-2-yl)-2-methoxyphenol (3d)*:** Yield 44%; m.p. 244–246 °C; FT-IR (KBr) υ (cm^{-1}): 3063 (O-H), 2972 (C-H),1585 (C=N), 1386 (C-N), 1228 (C-F), 1249, 1024 (C-O-C); ^{1}H NMR (400 MHz, DMSO-d_6): δ 9.047 (s, 1H, ArOH), 8.233 (d, 1H, J=9.44 Hz, ArH), 8.0 (d, 1H, J=7.9 Hz, ArH), 7.36–7.33 (m, 2H, ArH), 7.24–7.16 (m, 3H, ArH), 7.09 (s, 1H, ArH), 6.9 (d, 1H, J=8.28 Hz, ArH), 6.73 (d, 1H, J=8.24 Hz, ArH), 3.66 (s, 3H, OCH_3); MS-API: $[M+H]^+$ 336 (Calcd. 335.11).

***5-(3-(4-Fluorophenyl)-3H-imidazo[4,5-b]pyridin-2-yl)-2-methoxyphenol (3e)*:** Yield 85%; m.p. 190–192 °C; FT-IR (KBr) υ (cm^{-1}): 3117 (O-H), 2964 (methyl C-H), 1606 (C=N), 1363 (C-N), 1228 (C-F), 1253, 1026 (C-O-C); ^{1}H NMR (400 MHz, DMSO-d_6): δ 8.97 (s, 1H, ArOH), 8.28 (d, 1H, J=4.8 Hz, ArH), 8.06 (d, 1H, J=7.96 Hz, ArH), 7.43–7.40 (m, 2H, ArH), 7.31–7.24 (m, 3H, ArH), 7.16 (s, 1H, ArH), 7.091 (s, 1H, ArH), 6.95 (d, 1H, J=8.16 Hz, ArH), 6.82 (d, 1H, J=8.48 Hz, ArH), 3.86 (s, 3H, OCH_3); MS-API: $[M+H]^+$ 336 (Calcd. 335.11).

***3-(4-Chlorophenyl)-2-(3-(trifluoromethyl)phenyl)-3H-imidazo[4,5-b]pyridine (3f)*:** Yield 68%; m.p. 220–223 °C; FT-IR (KBr) υ (cm^{-1}): 3045 (aromatic C-H), 1591 (C=N), 1383 (C-N), 1329 (C-F, CF_3), 1095 (C-Cl); ^{1}H NMR (400 MHz, DMSO-d_6): δ 8.43 (d, 1H, J=4.8 Hz, ArH), 8.18 (d, 1H, J=8.0 Hz, ArH), 8.02 (s, 1H, ArH), 7.67 (t, 2H, J=8.12 Hz, ArH), 7.54–7.45 (m, 3H, ArH), 7.37–7.32 (m, 3H, ArH); MS-API: $[M+H]^+$ 374 (Calcd. 373.06).

***3-(4-Chlorophenyl)-2-(3,4,5-trimethoxyphenyl)-3H-imidazo[4,5-b]pyridine (3g)*:** Yield 88%; m.p. 193–195 °C; FT-IR (KBr) υ (cm^{-1}): 3024 (aromatic C-H), 2962 (methyl C-H), 1587 (C=N), 1373 (C-N), 1240, 1010 (C-O-C), 1089 (C-Cl); ^{1}H NMR (400 MHz, DMSO-d_6): δ 8.31 (d, 1H, J=4.88 Hz, ArH), 8.07 (d, 1H, J=8.0 Hz, ArH), 7.47–7.44 (m, 2H, ArH), 7.32–7.29 (m, 2H, ArH), 7.26–7.23 (m, 1H, ArH), 6.75 (s, 2H, ArH), 3.81 (s, 3H, OCH_3), 3.63 (s, 6H, OCH_3); MS-API: $[M+H]^+$ 396 (Calcd. 395.1).

***5-(3-(3,4-Dimethoxyphenyl)-3H-imidazo[4,5-b]pyridin-2-yl)-2-methoxyphenol (3h)*:** Yield 52%; m.p. 193–195 °C; FT-IR (KBr) υ (cm^{-1}): 3200 (O-H), 3066 (C-H aromatic), 2945 (methyl C-H), 1597 (C=N), 1384 (C-N), 1240, 1018 (C-O-C); ^{1}H NMR (400 MHz, DMSO-d_6): δ 8.35 (d, 1H, J=4.84Hz, ArH), 8.11 (d, 1H, J=8.0 Hz, ArH), 7.29–7.26 (m, 3H, ArH), 6.99 (s, 2H, ArH), 6.84 (s, 1H, ArH), 6.79 (d, 1H, J = 8.52 Hz, ArH) 3.95 (s, 3H, OCH_3), 3.88 (s, 3H, OCH_3), 3.8 (s, 3H, OCH_3); MS-API: $[M+H]^+$ 378 (Calcd. 377.14).

4.2. *Pharmacology*

4.2.1. *Cytotoxicity studies*

Lung cancer cell line A549, colon carcinoma cell line HCT-15, breast carcinoma cell lines MDA-MB-231 and MDA-MB-468,

prostatic cancer cell line DU-145, pancreatic cancer cell line PANC-1, human embryonic kidney cells HEK293, and mouse fibroblast KB-31 were grown as adherent monolayers in flasks with Dulbecco's modified Eagle's medium (DMEM) supplemented with 10% fetal bovine serum (FBS) in a humidified incubator containing 5% CO_2 at 37 °C. The human cancerous cell lines MCF-7 (breast cancer), SaOS-2 (osteosarcoma), and K562 (myelogenous leukemia) were maintained in Eagle's minimal essential medium, McCoy's 5a medium and RPMI-1640, respectively, and supplemented with $NaHCO_3$, sodium pyruvate, 10% fetal calf serum, and 1% penicillin and streptomycin. These cells were grown at 37 °C, 5% CO_2 in a humidified air.

The MTT assay was used to determine the cytotoxicity of the compounds to the following cells: HCT-15, MCF-7, MDA-MB-231, MDA-MB-468, SaOS-2, K562, DU-145, PANC-1, HEK293, and KB-31. Briefly, the cells used in this study were harvested with trypsin and suspended at a final concentration of 5×10^3 cells in each well. Cells were seeded (180 µL/well) into 96-well multiplates. Different concentrations of each compound in the series (20 µL) were added. After 72 h of incubation, 20 µL of the MTT solution (4 mg/mL) was added to each well, and the plates were incubated for 4 h. This allowed viable cells to convert the yellow-colored MTT into dark-blue formazan crystals. Subsequently, the medium was discarded, and 100 µL of DMSO was added into each well to dissolve the formazan crystals. The absorbance was determined at 570 nm with a DTX 880 multimode detector. The mean ± SD concentrations were calculated from 2 to 3 experiments performed in triplicate. The IC_{50} values were calculated from the cell survival percentages.

4.2.2. *Assays for COX-1 and COX-2 inhibition*

COX-1 has been isolated from Ram seminal vesicles. Recombinant human COX-2 has been expressed in an insect cell expression system. These enzymes have been purified by employing conventional chromatographic techniques. Enzymatic activities of COX-1 and COX-2 were measured according to the method[13] with slight modifications using a chromogenic assay based on the oxidation of *N,N,N′,N′*,-tetramethyl-*p*-phenylene diamine (TMPD) during the reduction of PGG2 to PGH2[14,15]. Briefly, the assay mixture containing Tris HCl buffer (100 mmol/L, pH 8.0), hematin (15 mmol/L), EDTA (3 mmol/L), enzyme (100 mg COX-1 or COX-2) and the test compound were pre-incubated at 25 °C for 1 min and then the reaction was initiated by the addition of arachidonic acid and TMPD, in total volume of 1 mL. The enzyme activity was determined by estimating the velocity of TMPD oxidation for the first 25 s of the reaction by following the increase in absorbance at 603 nm. A low rate of non-enzymatic oxidation observed in the absence of COX-1 and COX-2 was subtracted from the experimental value while calculating the percent inhibition.

4.3. *Molecular docking studies*

The docking analysis of most active molecule was performed using Maestro (version 9.2; Schrödinger, LLC: New York, NY, USA, 2012). The molecules were sketched in 3D format using build panel and LigPrep module was used to produce low-energy conformers. The structural coordinates of COX-2[16] was obtained from protein data bank. The protein was prepared by giving preliminary treatment like adding hydrogen atoms, adding missing residues, refining the loop with prime and finally minimized using the OPLS-2005 force field. Grid for molecular docking was generated with bound co-crystallized ligand (celecoxib). The molecules were docked using Glide (version 5.7; Schrödinger, LLC: New York, NY, 2012) in the extra-precision mode, with up to three poses saved. Ligands were kept flexible by producing the ring conformations and by penalizing non-polar amide bond conformations, whereas the receptor was kept rigid throughout the docking studies. All other parameters of the Glide module were maintained at their default values. The lowest energy conformation was selected for the prediction of ligand interactions with the active sites of COX-2.

Acknowledgments

The authors gratefully acknowledge the Sophisticated Analytical Instrumentation Facility, Indian Institute of Technology, Delhi, India for the NMR spectral analysis of the compounds used in this study. The authors Tarun Batra and Deepak Chowrasia are the recipients of GPAT scholarship offered by All India Council of Technical Education, New Delhi, India. We thank Ms. Charisse Montgomery, University of Toledo for editing this manuscript in the present form.

References

1. Smith DA. In: *Metabolism, pharmacokinetics and toxicity of functional groups: impact of the building blocks of medicinal chemistry in ADMET*. Cambridge: Royal Society of Chemistry; 2010.
2. Koyama Nobuhiro, Sato Hirofumi, Tomoda Hiroshi. Discovery of new hazimycin congeners from Kitasatospora sp. P07101. *Acta Pharm Sin B* 2015;**6**:564–8.
3. Manivannan E, Chaturvedi SC. Analogue-based design, synthesis and molecular docking analysis of 2,3-diaryl quinazolinones as non-ulcerogenic anti-inflammatory agents. *Bioorg Med Chem* 2011;**19**:4520–8.
4. Romagnoli R, Baraldi PG, Cruz-Lopez O, Lopez Cara C, Carrion MD, Brancale A, et al. Synthesis and antitumor activity of 1,5-disubstituted 1,2,4-triazoles as *cis*-restricted combretastatin analogues. *J Med Chem* 2010;**53**:4248–58.
5. Ohsumi K, Hatanaka T, Fujita K, Nakagawa R, Fukuda Y, Nihei Y, et al. Syntheses and antitumor activity of *cis*-restricted combretastatins: 5-membered heterocyclic analogues. *Bioorg Med Chem Lett* 1998;**8**:3153–8.
6. Wang L, Woods KW, Li Q, Barr KJ, McCroskey RW, Hannick SM, et al. Potent, orally active heterocycle-based combretastatin A–4 analogues: synthesis, structure−activity relationship, pharmacokinetics, and *in vivo* antitumor activity evaluation. *J Med Chem* 2002;**45**:1697–711.
7. Tron GC, Pagliai F, Del Grosso E, Genazzani AA, Sorba G. Synthesis and cytotoxic evaluation of combretafurazans. *J Med Chem* 2005;**48**:3260–8.
8. Kaffy J, Pontikis R, Carrez D, Croisy A, Monneret C, Florent JC. Isoxazole-type derivatives related to combretastatin A–4, synthesis and biological evaluation. *Bioorg Med Chem* 2006;**14**:4067–77.
9. Wu MJ, Sun QM, Yang CH, Chen DD, Ding J, Chen Y, et al. Synthesis and activity of combretastatin A–4 analogues: 1,2,3-thiadiazoles as potent antitumor agents. *Bioorg Med Chem Lett* 2007;**17**:869–73.
10. Odlo K, Hentzen J, dit Chabert JF, Ducki S, Gani OABSM Sylte I, et al. 1,5-Disubstituted 1,2,3-triazoles as *cis*-restricted analogues of combretastatin A–4: synthesis, molecular modeling and evaluation as cytotoxic agents and inhibitors of tubulin. *Bioorg Med Chem* 2008;**16**:4829–38.
11. Almansa C, de Arriba AF, Cavalcanti FL, Gómez LA, Miralles A, Merlos M, et al. Synthesis and SAR of a new series of COX-2-

selective inhibitors: pyrazolo[1,5-*a*]pyrimidines. *J Med Chem* 2001;**44**:350–61.

12. Yang DL, Fokas D, Li JZ, Yu LB, Baldino CM. A versatile method for the synthesis of benzimidazoles from *o*-nitroanilines and aldehydes in one step *via* a reductive cyclization. *Synthesis* 2005;**2005**:47–56.
13. Copeland RA, Williams JM, Giannaras J, Nurnberg S, Covington M, Pinto D, et al. Mechanism of selective inhibition of the inducible isoform of prostaglandin G/H synthase. *Proc Natl Acad Sci U S A* 1994;**91**:11202–6.
14. Egan RW, Paxton J, Kuehl Jr. FA. Mechanism for irreversible self-deactivation of prostaglandin synthetase. *J Biol Chem* 1976;**251**:7329–35.
15. Pagels WR, Sachs RJ, Marnett LJ, Dewitt DL, Day JS, Smith WL. Immunochemical evidence for the involvement of prostaglandin H synthase in hydroperoxide-dependent oxidations by ram seminal vesicle microsomes. *J Biol Chem* 1983;**258**:6517–23.
16. Wang JL, Limburg D, Graneto MJ, Springer J, Hamper JRB, Liao SB, et al. The novel benzopyran class of selective cyclooxygenase-2 inhibitors. Part 2: the second clinical candidate having a shorter and favorable human half-life. *Bioorg Med Chem Lett* 2010;**20**:7159–63.